ARTICLE

Polymer-Derived Ceramic Composite Fibers with Aligned Pristine Multiwalled Carbon Nanotubes

Sourangsu Sarkar,[†,‡] Jianhua Zou,[†] Jianhua Liu,[†] Chengying Xu,[§] Linan An,[*,||] and Lei Zhai[*,†,‡]

NanoScience Technology Center, Department of Chemistry, Advanced Materials Processing and Analysis Center, and Department of Mechanical, Materials and Aerospace Engineering, University of Central Florida, Orlando, Florida 32826

ABSTRACT Polymer-derived ceramic fibers with aligned multiwalled carbon nanotubes (MWCNTs) are fabricated through the electrospinning of polyaluminasilazane solutions with well-dispersed MWCNTs followed by pyrolysis. Poly(3-hexylthiophene)-*b*-poly (poly (ethylene glycol) methyl ether acrylate) (P3HT-b-PPEGA), a conjugated block copolymer compatible with polyaluminasilazane, is used to functionalize MWCNT surfaces with PPEGA, providing a noninvasive approach to disperse carbon nanotubes in polyaluminasilazane chloroform solutions. The electrospinning of the MWCNT/polyaluminasilazane solutions generates polymer fibers with aligned MWCNTs where MWCNTs are oriented along the electrospun jet by a sink flow. The subsequent pyrolysis of the obtained composite fibers produces ceramic fibers with aligned MWCNTs. The study of the effect of polymer and CNT concentration on the fiber structures shows that the fiber size increases with the increment of polymer concentration, whereas higher CNT content in the polymer solutions leads to thinner fibers attributable to the increased conductivity. Both the SEM and TEM characterization of the polymer and ceramic fibers demonstrates the uniform orientation of CNTs along the fibers, suggesting excellent dispersion of CNTs and efficient CNT alignment via the electrospinning. The electrical conductivity of a ceramic fibers with 1.2% aligned MWCNTs is measured to be 1.58×10^{-6} S/cm, which is more than 500 times higher than that of bulk ceramic (3.43×10^{-9} S/cm). Such an approach provides a versatile method to disperse CNTs in preceramic polymer solutions and offers a new approach to integrate aligned CNTs in ceramics.

KEYWORDS: align • carbon nanotubes • polymer-derived ceramic • electrospun fibers

INTRODUCTION

Incorporating carbon nanotubes (CNTs) in polymeric (1–3), metallic (4), metal-ceramic (5, 6), and ceramic (7–13) matrices can significantly improve their mechanical, electrical, or thermal properties. Furthermore, various interesting anisotropic properties can be obtained by aligning CNTs in matrices because CNTs have extremely high aspect ratios (length/diameter), with diameters of one to tens of nanometers and lengths up to micrometers, or even centimeters (14, 15). For example, CNTs have been aligned in various polymer matrices to achieve anisotropic electrical conductance (16, 17), anisotropic thermal diffusivity (18), and unidirectional reinforcement (19). Integrating aligned CNTs in ceramic materials is important for applications including rocket nozzles and hot gas filters where requirements such as strength, stiffness, and resistance to corrosion prevent the use of polymer or metals. However, the utilization of CNT anisotropic properties in ceramics is limited by the availability of appropriate ceramic materials, effective dispersion, and alignment of CNTs in matrices. It is a formidable challenge to achieve proper dispersion and alignment of CNTs in ceramics by conventional powder-based processing techniques. To disperse and align CNTs in ceramic matrices, it is necessary to have a solution processable ceramic precursor and a suitable CNT dispersant that is compatible with the ceramic precursor. Polymer-derived ceramics (PDCs), unlike conventional ceramics obtained by sintering method, are synthesized by direct thermal decomposition of polymeric precursors (20, 21). This unique direct polymer to ceramics route makes PDCs suitable for fabrication of different unconventionally shaped ceramic components and devices (22, 23). For example, one-dimensional PDC nanostructures, such as nanowires, nanotubes, and nanorods, have been fabricated by using the off-gases from PDC preparation and via a template approach (24, 25). Our group has developed a unique simple technique to synthesize ceramic fibers via the electrospinning of aluminum functionalized oligosilazane. Preceramic polymer (polyaluminasilazane) fibers were fabricated via the electrospinning of polymer solutions. The following pyrolysis of the polymer fibers at 1000 °C in Ar produced SiCNAl ceramic fibers (26). To disperse CNTs in various solvents and polymer matrices, Zou and co-workers have developed a novel approach a series of dispersants based on using conjugated block copolymers (27, 28). This approach does not require any

* Corresponding author. E-mail: lzhai@mail.ucf.edu (L.Z.); lan@mail.ucf.edu (L.A.).

Received for review January 4, 2010 and accepted March 15, 2010

[†] NanoScience Technology Center, University of Central Florida.

[‡] Department of Chemistry, University of Central Florida.

[§] Department of Mechanical, Materials and Aerospace Engineering, University of Central Florida.

[||] Advanced Materials Analysis and Processing Center, University of Central Florida.

DOI: 10.1021/am1000085

Published on Web 03/29/2010

Scheme 1. (a) Structure of Oligosilazane and (b) Synthesis Scheme of P3HT-b-PPEGA

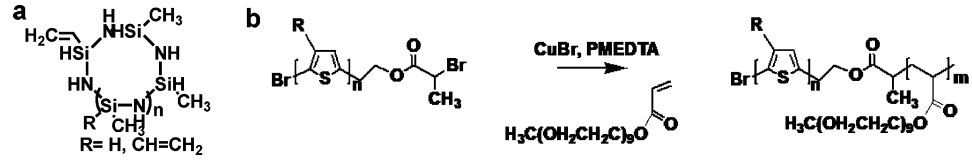

invasive chemical functionalization of CNT surfaces, which deteriorates the electrical and mechanical properties of CNTs. With a simple ultrasonication, the conjugated polymer block such as poly(3-hexyltiophene) (P3HT) can form strong $\pi-\pi$ interactions with nanotube walls, whereas nonconjugated polymer block with tunable composition will provide the debundled CNTs with good solubility and stability in a wide range of organic solvents and host polymer matrices. These research results provide suitable ceramic matrices and CNT dispersants to incorporate aligned CNTs in ceramics.

Among various existing approaches to align dispersed CNTs including mechanical stretching (29), assembling under magnetic (30, 31) and electric fields (32), electrospinning has been widely used because of its ease and flexibility in operation. In a typical electrospinning process, a high electrostatic force is applied to a solution held in a syringe with a needle. A jet is emitted from the conelike meniscus (Taylor cone) formed on the needle tip when the field strength exceeds a critical value to overcome the polymer solution surface tension. As the jet moves toward the collecting electrode, its diameter decreases because of lateral excursions, and the solvent evaporates, leading to a nonwoven fabric mat on the collecting electrode (33–35). Various polymer fibers containing aligned CNTs have been fabricated by electrospinning polymer solutions containing dispersed CNTs (36–45), where CNTs lined up during the electrospinning process because of the sink flow and high extension of the electrospun jet (46).

On the basis of the achievement in the material development and well-established electrospinning technology, we rationalized that ceramic fibers with aligned CNTs could be fabricated by pyrolyzing CNT/preceramic polymer electrospun fibers produced from preceramic polymer solutions with CNTs dispersed by conjugated block copolymers. In this paper, we report the fabrication of ceramic fibers with aligned CNTs from preceramic polymer solutions containing dispersed multiwalled carbon nanotubes (MWCNT). MWCNTs were dispersed uniformly by a conjugated block copolymer-poly(3-hexylthiophene)-*b*-poly (poly (ethylene glycol) methyl ether acrylate) (P3HT-*b*-PPEGA) in chloroform solutions of polyaluminasilazane, a synthesized solution-processable preceramic polymer. SiCNAl ceramic fibers with aligned MWCNTs were fabricated through the electrospinning of CNT/polyaluminasilazane solutions followed by a pyrolysis of the obtained fibers. The effect of polymer solution concentration and MWCNT/polymer ratio on fiber structures is discussed. The alignment of CNT in ceramic fibers and the improvement of the electrical conductivity by the aligned CNTs are demonstrated. Such an approach provides a versatile method to disperse CNTs in preceramic polymer solutions and offers a new approach to integrate aligned CNTs in ceramics.

EXPERIMENTAL METHOD

Synthesis of Polyaluminasilazane and Block Copolymer Poly(3-hexylthiophene)-*b*-poly (poly(ethylene glycol) methyl ether acrylate) (P3HT-*b*-PPEGA) (Scheme 1). Solid preceramic polyaluminasilazane was synthesized from Ceraset VL 20 according to our previously reported procedure (26) (see the Supporting Information). The block copolymer, P3HT-*b*-PPEGA, was synthesized according to the literature procedure reported by Zou et al. (27) (see Figures S2 and S3 in the Supporting Information for reaction scheme and ^{1}H NMR characterization).

Dispersion of MWCNTs in Polyaluminasilazane Solutions. MWCNTs were purchased from Nanolab (Newton, MA) with a diameter of 10−20 nm and a length of 5−20 μm (The purity is above 95%). The as-received CNTs were used without any further purification or chemical modification; 1 mg/mL CNT dispersion in $CHCl_3$ with P3HT-*b*-PPEGA was prepared by adding 10 mg of CNT and 20 mg of P3HT-*b*-PPEGA in 10 mL of $CHCl_3$ followed by ultrasonication for 1 h with the water bath temperature maintained at 0−10 °C. Twenty-percent polyaluminasilazane solution containing 0.2% CNT with respect to polyaluminasilazane was prepared by mixing 1.5 g of the above prepared CNT/$CHCl_3$ dispersion with 0.5 g of polyaluminasilazane and 0.5 g of 1% polyethylene oxide (PEO, $M_n = 1\,000\,000$, purchased from Sigma-Aldrich, St. Louise, MO). The ratio of polyaluminasilazane to PEO was maintained at 100. The mixture was sonicated for 5 min.

Electrospinning MWCNT/Polyaluminasilazane Composite Solutions and Pyrolysis. In a typical electrospinning procedure, the CNT/Polyaluminasilazane/PEO solution was loaded in a 5 mL disposable syringe equipped with a stainless steel needle connected to high voltage supply (Glassman High Voltage Inc., High Bridge, NJ). The solution was electrospun at 10 kV with a feed rate of 0.3 mL/h using a syringe pump (New Era Pump Systems Inc., Wantagh, NY). The electrospun fibers were collected on a silicon (Si) wafer at a collector distance of 24.0 cm. The obtained fibers were pyrolyzed at 1000 °C for 1 h in a tube furnace under an Ar atmosphere at a heating rate of 5 °C/min to produce ceramic fibers.

Fabrication of Platinum (Pt) Electrodes. Single ceramic fibers were drop-cast on a gold (Au) electrode-patterned SiO_2/Si substrate from their ethanol dispersion. Two Pt electrodes were deposited on a fiber with a distance of approximately 100 μm and connected to the adjacent Au electrodes by focused ion beam (FIB) technique.

Characterization. ^{1}H NMR of the block copolymer P3HT-*b*-PPEGA and polyaluminasilazanes were acquired on a Varian Mercury Gemini Spectrometer at 500 MHz using $CDCl_3$ as the solvent. The molecular weight of the block copolymer was determined using JASCO Gel Permeation Chromatography system (JASCO Inc., Easton, MD) with ultraviolet, refractive index and static light scattering detectors. The surface morphology of the electrospun fibers and the surface composition of the Pt deposited fibers were examined by Zeiss Ultra-55 FEG scanning electron microscope (SEM) equipped with Noran System 7 EDS with silicon drift X-ray detector. The orientation of the MWCNTs in the fibers was characterized by FEI Technai

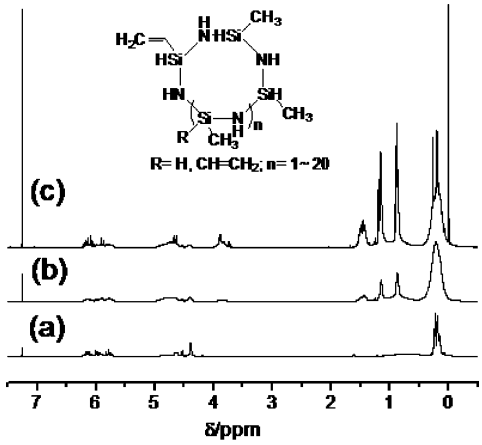

FIGURE 1. ^{1}H NMR of (a) Ceraset VL 20, (b) 15% Al sec-butoxide treated Ceraset VL 20, and (c) 30% Al sec-butoxide treated Ceraset VL 20.

F30 transmission electron microscope (TEM). Thin specimens for TEM were prepared by FIB etching of the fibers using FEI 200 TEM FIB using gallium as the liquid metal ion source followed by ex-situ deposition of the specimen on carbon coated copper TEM grids. Raman spectra of the composite fibers were obtained using Renishaw Raman Microscope (Renishaw Inc., Gloucestershire, U.K.) at 785 nm silicon-solid laser excitation source. Room temperature *I*−*V* characteristics of the fiber were measured using a two-probe Keithley-238 source-measure unit.

RESULTS AND DISCUSSION

The preceramic polymer used in this study is produced from a commercially available cyclosilazane known as Ceraset VL 20. Ceraset VL 20 is a low molecular weight (average molecular weight around 300) liquid oligosilazane, and can not be directly used for electrospinning (47). In our previous studies, a solid polyaluminasilazane was synthesized by a treatment of Ceraset VL 20 with aluminum trisec-butoxide. It is hypothesized that the coupling reaction between aluminum and nitrogen could be the reason for the transformation from liquid oligosilazane to solid polyaluminasilazane. To corroborate the hypothesis, we investigated the reaction mechanism using ^{1}H NMR spectroscopy. ^{1}H NMR spectra of Ceraset VL20 (Figure 1a) shows four characteristics peaks, which can be assigned to Si−CH=CH_2 (5.73−6.17 ppm), Si−H (4.42−5.02 ppm), N−H (0.82−0.89 ppm), and Si−CH_3 (0.09−0.33 ppm). It is believed that Ceraset VL20 became partially cross-linked because of the hydrosilylation between Si−H and Si−CH=CH_2 groups at lower temperatures. Therefore, the estimated conversion of Si−H groups by the treatment of Ceraset VL20 with varying amounts of aluminum sec-butoxide at the same reaction conditions could be an efficient route to predict the reaction pathway. To our expectation, the conversion of Si−H was calculated to be 18% and 5% for 15% and 30% Al sec-butoxide treated Ceraset VL20, respectively (Figure 1b,c). The decrease in Si−H conversion with increasing aluminum content suggests that the Lewis acid−base complexation reaction between aluminum and nitrogen and the presence of bulky trisec-butoxide groups prevents the cross-linking of Ceraset VL20 via hydrosilylation, and favors the formation of a solvent-soluble solid complex.

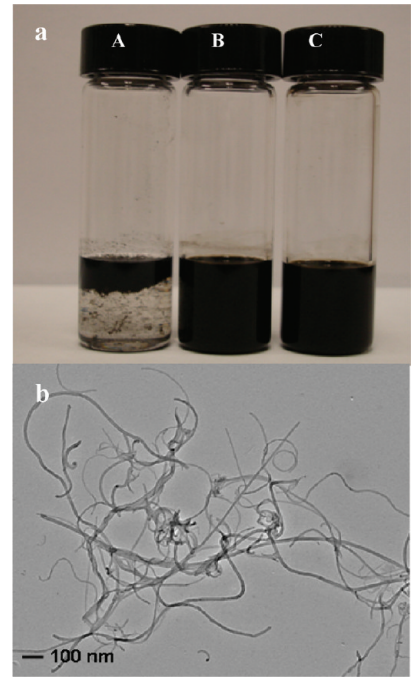

FIGURE 2. (a) Photographs of (A) MWCNT agglomeration in polyaluminasilazane/$CHCl_3$ solution, (B) P3HT-*b*-PPEGA dispersed MWCNTs in $CHCl_3$, (C) P3HT-*b*-PPEGA dispersed MWCNTs in polyaluminasilazane/PEO chloroform solutions; (b) TEM image of MWCNT dispersed in a polysilazane/P3HT-b-PPEGA/PEO chloroform solution.

The obtained polyaluminasilazane was soluble in common solvents such as chloroform ($CHCl_3$), tetrahydrofuran (THF) and *N*,*N*-dimethylformamide (DMF) and was electrospun into smooth fibers. SiCNAl with a composition of $Si_{1.0}C_{0.5}N_{0.4}Al_{0.07}O_{0.01}$ was obtained after pyrolyzing the polyaluminasilazane fibers (26). Incorporating CNTs into polyaluminasilazane requires a stable dispersion of the nanotubes in polyaluminasilazane solutions before electrospinning. However, pristine nanotubes form agglomerates in solvents like $CHCl_3$ without proper dispersion because of strong van der Waals interactions between the nanotubes (Figure 2a-A). To create stable CNT dispersion in polyaluminasilazane chloroform solutions, we synthesized an amphiphilic conjugated block copolymer, poly(3-hexylthiophene)-*b*-poly (poly (ethylene glycol) methyl ether acrylate) (P3HT-*b*-PPEGA), to produce a stable CNT dispersion in polyaluminasilazane chloroform solutions (27). The PPEGA block in P3HT-*b*-PPEGA has ethylene oxide groups like poly(ethylene oxide) (PEO) (48). Such a block copolymer is readily soluble in both polar and nonpolar solvents and expected to facilitate the dispersion of CNTs in polyaluminasilazane solutions. Indeed, P3HT-*b*-PPEGA is a sufficient dispersant to produce stable CNT dispersion in polyaluminasilazane chloroform solutions. The CNTs were uniformly dispersed in chloroform by P3HT-*b*-PPEGA (The ratio of CNT to P3HT-*b*-PPEGAA was 1:2; Figure 2a-B), generating a CNT dispersion (1 mg/mL) that was stable for several months. The addition of as-synthesized polyaluminasilazane did not disrupt the dispersion (Figure 2a-C). The transmission electron microscopy (TEM) characterization of the CNT dispersion in polyaluminasilazane chloroform solutions (Figure 2b) indicated that majority

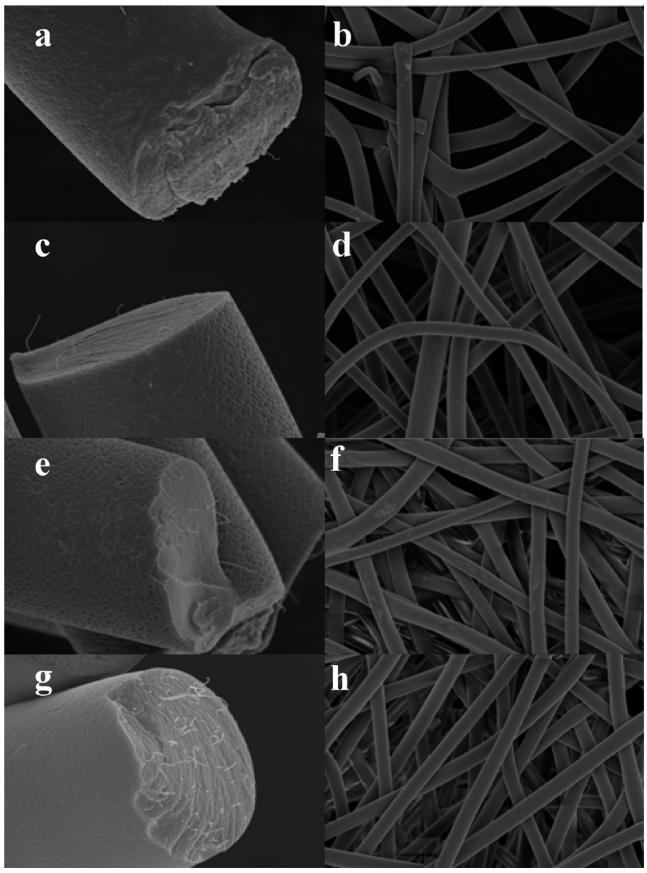

FIGURE 3. SEM images of electrospun fibers at different concentrations of MWCNT in 20% polyaluminasilazane solutions: (a, b) 0.025% MWCNT; (c, d) 0.05% MWCNT; (e, f) 0.1% MWCNT; (g, h) 0.2% MWCNT). The scale bar for a, c, e, and g is 2 μm and for b, d, f, and h is 10 μm. Fibers become regular in shape as the MWCNT concentration increases.

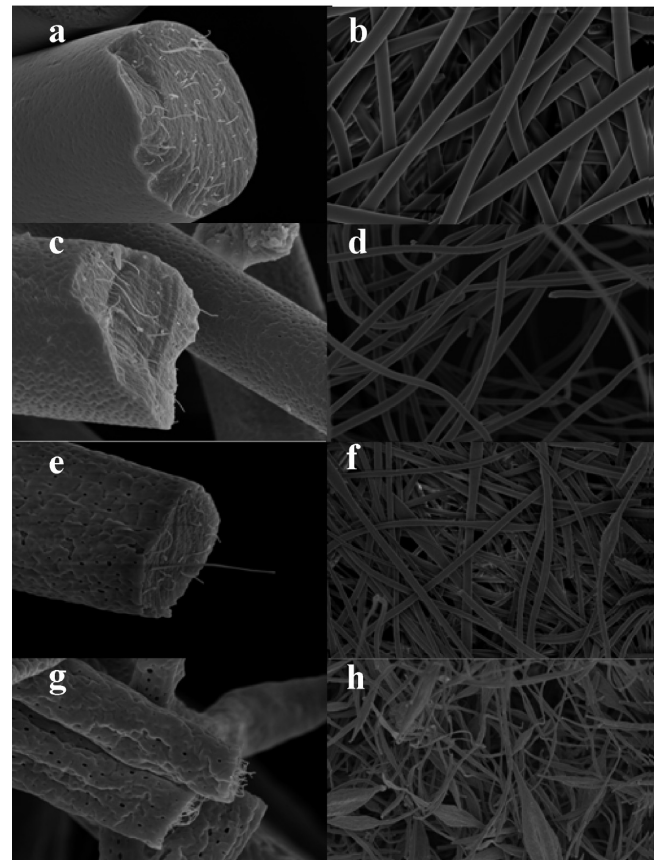

FIGURE 4. SEM images of electrospun fibers from different composition of polyaluminasilazane and MWCNT: (a, b) 20% polyaluminasilazane/0.2% MWCNT; (c, d) 15% polyaluminasilazane/0.3% MWCNT; (e, f) 10% polyaluminasilazane/0.5% MWCNT; (g, h) 5% polyaluminasilazane/1.2% MWCNT). The scale bar for a, c, e, and g is 2 μm and for b, d, f, and h is 10 μm.

of the nanotubes are debundled and dispersed into individual tubes.

Electrospinning of the CNT/polyaluminasilazane solutions generated droplets due to insufficient chain entanglement among short polyaluminasilazanes and block copolymer P3HT-b-PPEGA polymer chains (49). To introduce sufficient chain entanglement and facilitate the fiber formation, small amount of high molecular PEO (M_n = 1 000 000) (the ratio of polyaluminasilazane to PEO was 100) was added to the polyaluminasilazane solution (50). Figure S2 in the Supporting Information shows the eletrospun cottonlike fibers formed from pure polyaluminasilazane and CNT/polyaluminasilazane chloroform solutions. The color of the CNT/polyaluminasilazane electrospun fibers is gray because CNTs are embedded in the fibers.

The effect of MWCNT concentration on electrospun fiber morphology was investigated using 20% polyaluminasilazane solutions with different CNT content (0.025−0.2% related to solid polymer). The scanning electron microscopy (SEM) images (Figure 3) show that the fibers become smoother and more regular as the CNT concentration increases, possibly because of the increasing chain entanglement induced by CNTs. The PPEGA blocks of P3HT-*b*-PPEGA attaching to CNT surfaces have similar structures to PEO with −OH groups at the ends, and interact with PEO (−OH groups at the ends) and polyaluminasilazane (−NH groups) through hydrogen bonding (48–50), introducing a higher degree of chain entanglement with more P3HT-*b*-PPEGA dispersed CNTs. Such a higher degree of chain entanglement increases the viscoelasticity of the solution (51, 52), resulting in smooth and uniform fibers. The fiber diameter change with CNT concentrations (0.025−0.2%) is not obvious in Figure 3. Such observation is unlike the reported effect of CNT concentration on electrospun fiber diameter where the solution conductivity increased with an increment of CNT concentration, generating higher charge density on the solution and producing thinner fibers (36). Such trivial effect of CNT concentration on electrospun fiber diameter is probably due to the low CNT concentration that is unable to introduce large conductivity change in solutions. When the CNTs concentration is high enough to increase the solution conductivity, the effect of the CNTs concentration on spun fiber diameter is observable. For example, the CNT/polyaluminasilazane fibers (4 μm) spun from 20% CNT/polyaluminasilazane (0.2% CNT related to solid polymer) solutions (Figure 4a) is thinner than the pure polyaluminasilazane fibers (5 μm) spun from 20% polyaluminasilazane solutions (see Figure S3 in the Supporting Information). Figure 4

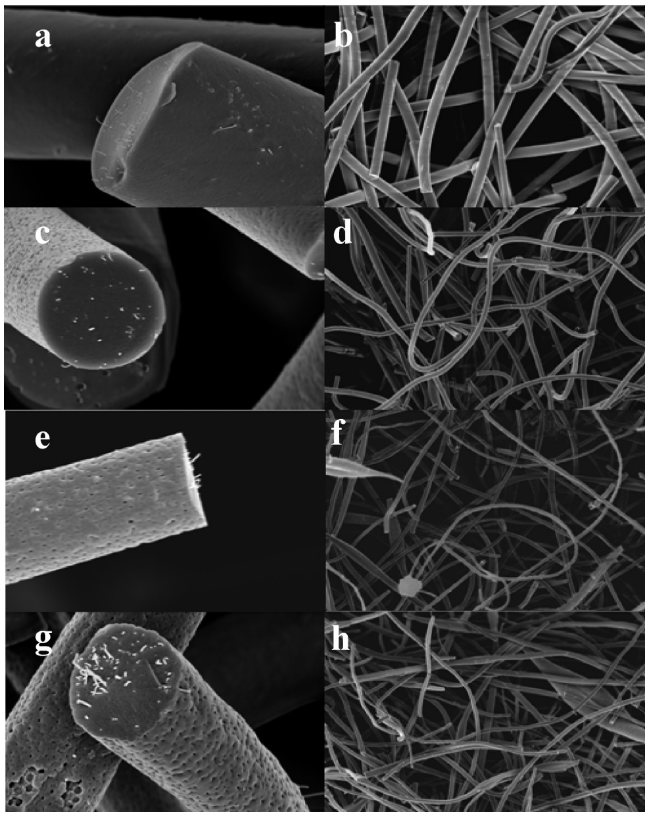

FIGURE 5. SEM images of pyrolyzed ceramic fibers from different composition of polyaluminasilazane and MWCNT: (a, b) 20% polyaluminasilazane/0.2% MWCNT; (c, d) 15% polyaluminsilazane/0.3% MWCNT; (e, f) 10% polyaluminasilazane/0.5% MWCNT; (g, h) 5% polyaluminsilazane/1.2% MWCNT. The scale bar for a, c, e, and g is 2 μm and for b, d, f, and h is 10 μm.

shows the SEM images of the CNT/polyaluminasilazane electrospun fibers from the composite solutions of polyaluminasilazane and CNT at different concentrations. The fiber diameter decreases from about 4 to 1 μm as the polyaluminasilazane concentration reduces from 20% to 5% and the nanotube concentration increases from 0.2% to 1.2%. This observation is in good agreement with our previous studies of the effect of polyaluminasilazane concentration on the size of electrospun fibers, showing that the fiber diameter increases with the increasing of polymer concentration. The fibers become rough, porous, and irregular in shape as the polymer content decreases. The formation of the pores is possibly caused by the condensation of moistures during the electrospinning process as explained by a "breath figure" model (53). During the electrospinning, the temperature of spinning jet drops with the evaporation of solvents, which causes the ambient moisture to condense onto the fiber surface. The condensed water droplets form pores when the solvent and water evaporates completely to generate solid fibers. The roughening of the fibers at high CNT concentration is possibly due to the increased electric field caused by the high electrical conductivity of CNT in the polymer solution (42).

The microscopic distribution of the CNTs in the composite fibers was investigated by examining the fractured surface of the fibers by SEM. Individual CNTs are protruding out of the fractured surface with a density increased with CNT concentration, suggesting excellent dispersion of CNTs by P3HT-*b*-PPEGA and good orientation of nanotubes along the fiber axis. The CNT/polyaluminasilazane fibers were then pyrolyzed at 1000 °C for an hour under Ar atmosphere. SEM images (Figure 5) of the SiCNAl ceramic fibers show that the fiber structure and the aligned CNTs remain unchanged despite 28% shrinkage of the fiber during the pyrolysis (54).

To study the orientation of the CNTs inside the ceramic fibers, we characterized thin specimen of the fibers by transmission electron microscopy (TEM). Although TEM is an effective tool to observe the orientation of nanotubes in electrospun nanofibers (41, 44, 55), micrometer-sized ceramic fiber is not suitable for direct TEM imaging. Therefore, portions of the ceramic fibers were removed by a focused ion beam (FIB) using liquid gallium (Ga) ion source. The obtained thin ceramic fiber specimen (about 150 nm) was examined by TEM (Figure 6a–d). Figures 6a–c are the TEM images of different parts on a CNT/SiCNAl (0.3% CNT) ceramic fiber, whereas Figure 6d is a high-resolution TEM image of a single MWCNT inside the fiber. MWCNTs (15–20 nm in diameter) have a darker concentric tubular structure in the ceramic matrix compared to the uniform matrix. It is evident that MWCNTs align in a considerable length along the fiber axis. These observations suggest that CNTs are well dispersed in the solution and align parallel to the fiber axis because of sink flow and high extension forces exerted on the electrospun jet (46). Before an electric field is applied to the droplet of a CNT/polyaluminasilazane solution, the CNTs behave like rodlike particles that orient randomly in the droplet. During the electrospinning, when an electrical field is applied to the droplet and generates a Taylor cone, the sink flow, also known as Hamel flow (56) causes CNTs to gradually orient along the electrospun jet.

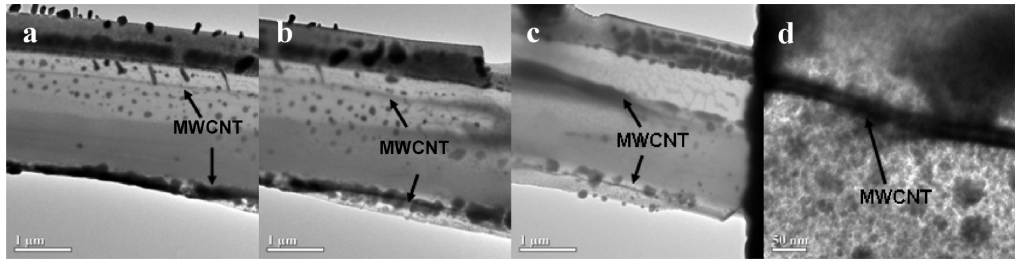

FIGURE 6. TEM images of (a–c) a FIB-cut 0.3% MWCNT/SiCNAl ceramic fiber, (d) MWCNT inside the ceramic fiber. (The scale bars for a–c is 1 μm and for d is 50 nm. The dark spots are the contaminants (Ga) deposited while thin fiber specimens were prepared for TEM by the FIB technique.)

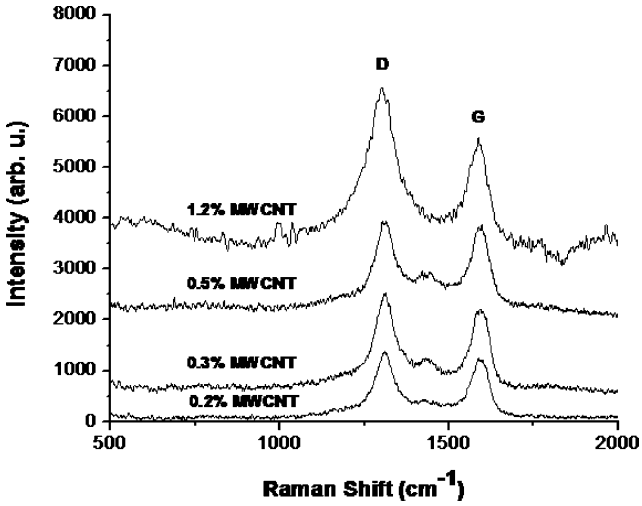

FIGURE 7. Raman spectra of the electrospun fibers with different weight percentages of MWCNTs. The intensity of the peaks decreases and shows a blue shift with the decrease in MWCNT concentrations.

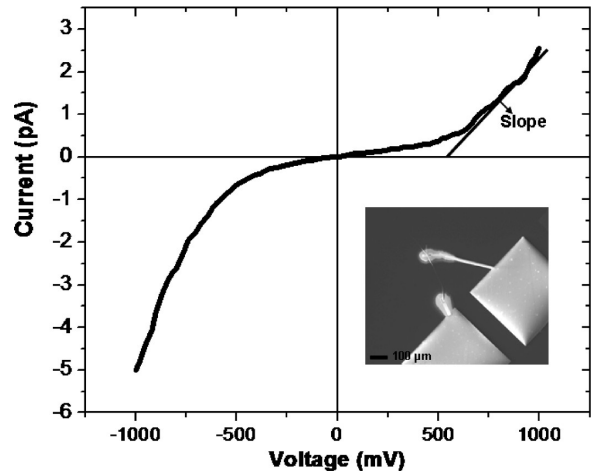

FIGURE 8. $I-V$ characteristics curve of a single MWCNT (1.2%)/SiCNAl ceramic fiber showing nonlinear behavior. The inset shows an image of a single fiber between two platinum (Pt) electrodes.

The alignment of the CNTs embedded in the electrospun fiber is strongly dependent on the quality of CNT dispersion (45). Electrospinning of the polymer solutions with poorly dispersed CNTs usually generate fibers with humps containing CNT aggregates (39). Aligned CNTs without any noticeable entanglement inside the ceramic fibers clearly illustrates the excellent dispersion of CNTs by P3HT-*b*-PPEGA and efficient alignment of CNT through electrospinning.

Raman spectroscopy was used to confirm the presence of aligned MWCNTs in polyaluminasilazane fibers (Figure 7). The MWCNTs embedded in polyaluminasilazane matrices show two strong characteristics peaks. The strong peak at 1302 cm^{-1}, D band, could be assigned as the disorder-induced features due to finite particle size effect or lattice distortion of graphitic crystals (41). The other strong peak at 1588 cm^{-1}, called G band, was due to the vibration of the sp^2 hybridized carbon atoms on the MWCNTs. The intensity of both peaks increases with increased MWCNT concentration, whereas the intensity ratio between the two peaks, I_D/I_G, remains constant. Also, the peaks show a little shift (6 to 9 cm^{-1}) toward the lower wave numbers as the MWCNT concentration increases from 0.2% to 1.2% (57).

To study the electrical properties of the MWCNT/SiCNAl ceramic fibers, we dispersed the fibers in ethanol by ultrasonication to obtain single fibers. The obtained single ceramic fibers were drop-cast onto an Au-patterned SiO_2/Si substrate. The single fiber chosen for $I-V$ measurement was close to the two adjacent Au electrodes. The fiber was then connected to these electrodes by the deposition of Pt using FIB. Since Ga metal is used in FIB as the ion source for imaging and Pt might be deposited along the fiber to make the fiber conductive, the elemental composition of the fiber surface were investigated by energy-dispersive spectroscopy (EDS) analysis. No trace of Ga and Pt contamination was found on the surface of the fiber after successful deposition of Pt electrodes, indicating that the electrical conductivity is solely from composite fibers. The $I-V$ characteristic of a single MWCNT (1.2%)/ceramic fiber (Figure 8) shows nonlinear behavior similar to that of MWCNT/poly(vinyl acetate) fibers (39). It is believed that the nonlinear characteristics of the $I-V$ curve of the MWCNT/ceramic composite fiber could arise from the intrinsic semimetallic nature of the MWCNT/ceramic composite, as well as could possibly be due to the contact resistance between the semiconductor−metal contact, typically known as Schottky contact. The dc conductivity of the MWCNT (1.2%)/ceramic fiber was measured from the slope of the linear region of the $I-V$ characteristics, as indicated in Figure 8. The obtained conductivity (1.58×10^{-6} S/cm) is more than 500 times higher than that of bulk SiCNAl ceramic (3.43×10^{-9} S/cm). This result suggests that the aligned nanotubes in ceramic fibers contribute to the increased electrical conductivity (58). The effects of CNT concentration on the electrical and mechanical properties of CNT/ceramic fibers is currently under investigation.

CONCLUSIONS

In summary, we have prepared MWCNT/SiCNAl ceramic fibers from polyaluminasilazane electrospun fibers with aligned CNTs. The effective dispersion of MWCNTs in polyaluminasilazane was achieved by using a conjugated block copolymer, P3HT-*b*-PPEGA. PPEGA groups on P3HT-*b*-PPEGA functionalized CNTs are compatible with polyaluminasilazane through hydrogen bonding and generate a stable dispersion of MWCNT in polyaluminasilazane solutions. Electrospinning of the MWCNT/polyaluminasilazane solutions produced polyaluminasilazane fibers with well-aligned CNTs. The pyrolysis of the obtained composite fibers generated SiCNAl ceramic fibers with aligned MWCNT. SiCNAl ceramic fibers with 1.2% MWCNTs have electrical conductivity 500 times higher than that of SiCNAl bulk samples, demonstrating the large improvement of electrical conductivity attributed to align CNTs. The reported method provides a versatile approach to disperse CNT in ceramics and paves a new path to align CNTs in ceramic fibers, which may find applications in ceramic matrix composites (CMC) with excellent electrical and mechanical properties.

Acknowledgment. Financial support from the National Science Foundation (DMR0706526) and help from Dr. Qi Zhang on TEM and FIB are gratefully acknowledged.

Supporting Information Available: Synthesis of poly-(3-hexylthiophene)-*b*-poly (poly (ethylene glycol) methyl ether acrylate), pictures of electrospun polyaluminasilazane and MWCNT/polyaluminasilazane (PDF). This material is available free of charge via the Internet at http://pubs.acs.org.

REFERENCES AND NOTES

(1) Coleman, J. N.; Khan, U.; Gun'Ko, Y. K. *Adv. Mater.* **2006**, *18*, 689–706.
(2) Moniruzzaman, M.; Winey, K. I. *Macromolecules* **2006**, *39*, 5194–5205.
(3) Ojha, S. S.; Afshari, M.; Kotek, R.; Gorga, R. E. *J. Appl. Polym. Sci.* **2008**, *108*, 308–319.
(4) Chen, W. X.; Tu, J. P.; Wang, L. Y.; Gan, H. Y.; Xu, Z. D.; Zhang, X. B. *Carbon* **2003**, *41*, 215–222.
(5) Laurent, Ch.; Peigney, A.; Dumoortier, O.; Rousset, A. *J. Eur. Ceram. Soc.* **1998**, *18*, 2005–2013.
(6) Peigney, A.; Laurent, Ch.; Dumoortier, O.; Rousset, A. *J. Eur. Ceram. Soc.* **1998**, *18*, 1995–2004.
(7) Padture, N. P. *Adv. Mater.* **2009**, *21*, 1767–1770.
(8) Solvas-Z, E.; Poyato, R.; Garcia, G. D.; Rodriguez, D. A.; Radmilovic, V.; Padture, N. P. *Appl. Phys. Lett.* **2008**, *92*, 111912−1111912−3.
(9) Woan, K.; Pyrgiotakis, G.; Sigmund, W. *Adv. Mater.* **2009**, *21*, 2233–2239.
(10) Gao, L.; Jiang, L.; Sun, J. *J. Electroceram.* **2006**, *17*, 51–55.
(11) Tatami, J.; Katashima, T.; Komeya, K.; Meguro, T.; Wakihara, T. *J. Am. Ceram. Soc.* **2005**, *88*, 2889–2893.
(12) Zhan, G.-D.; Kunitz, J. D.; Wan, J.; Mukherjee, A. K. *Nat. Mater.* **2003**, *2*, 38–42.
(13) Zhan, G.-D.; Kunitz, J. D.; Garay, J. E.; Mukherjee, A. K. *Appl. Phys. Lett.* **2003**, *83*, 1228–1230.
(14) Li, S.; Yu, Z.; Rutherglen, C.; Burke, P. J. *Nano Lett.* **2004**, *4*, 2003–2007.
(15) Zheng, L. X.; O'Connell, M. J.; Doorn, S. K.; Liao, X. Z.; Zhao, Y. H.; Akhadov, E. A.; Hoffbauer, M. A.; Roop, B. J.; Jia, Q. X.; Dye, R. C.; Peterson, D. E.; Huang, S. M.; Liu, J.; Zhu, Y. T. *Nat. Mater.* **2004**, *3*, 673–676.
(16) Yao, Y.; Liu, C.; Fan, S. *Nanotechnology* **2006**, *17*, 4374–4378.
(17) Adachi, N.; Fukawa, T.; Tatewaki, Y.; Shirai, H.; Kimura, M. *Macromol. Rapid Commun.* **2008**, *29*, 1877–1881.
(18) Borca-Tasciuc, T.; Mazumder, M.; Son, Y.; Pal, S. K.; Schadler, L. S.; Ajayan, P. M. *J. Nanosci. Nanotechnol.* **2007**, *7*, 1581–1588.
(19) Che, J.; Yuan, W.; Jiang, G.; Dai, J.; Lim, S. U.; Chan-Park, M. B. *Chem. Mater.* **2009**, *21*, 1471–1479.
(20) Riedel, R.; Passing, G.; Schonfelder, H.; Brook, R. J. *Nature* **1992**, *355*, 714–717.
(21) Kroke, E.; Li, Y. L.; Konetchny, C.; Lecomte, E.; Fasel, D.; Riedel, R. *Mater. Sci. Eng., R* **2004**, *26*, 197–199.
(22) Liew, L.; Zhang, W.; An, L.; Shah, S.; Lou, R.; Liu, Y.; Cross, T.; Anseth, K.; Bright, V.; Raj, R. *Am. Ceram. Soc. Bull.* **2001**, *80*, 25–30.
(23) An, L.; Xu, W.; Rajagopalan, S.; Wang, C.; Wang, H.; Kapat, J.; Chow, L.; Fan, Y.; Zhang, L.; Jiang, D.; Guo, B.; Liang, J.; Vaidyanathan, R. *Adv. Mater.* **2004**, *16*, 2036–2040.
(24) Pashchanka, M.; Engstler, J.; Schneider, J. J.; Siozios, V.; Fasel, C.; Hauser, R.; Kinski, I.; Riedel, R.; Lauterbach, S.; Kleebe, H.-J.; Flege, S.; Ensinger, W. *Eur. J. Inorg. Chem.* **2009**, *2009*, 3496–3506.
(25) Li, Y.-G.; Li, D.-X.; Wang, H.; Liu, L. *Appl. Phys. A: Mater. Sci. Process.* **2010**, *98*, 293–298.
(26) Sarkar, S.; Chunder, A.; Fei, W.; An, L.; Zhai, L. *J. Am. Ceram. Soc.* **2008**, *91*, 2751–2755.
(27) Zou, J.; Khondalker, S. I.; Huo, Q.; Zhai, L. *Adv. Funct. Mater.* **2009**, *19*, 479–483.
(28) Zou, J.; Liu, L.; Chen, H.; Khondaker, S. I.; McCullough, R.; Huo, Q.; Zhai, L. *Adv. Mater.* **2008**, *20*, 2055–2060.
(29) Jin, L.; Bower, C.; Zhou, O. *Appl. Phys. Lett.* **1998**, *73*, 1197–1199.
(30) Camponeschi, E.; Vance, R.; Marwan, A.-H.; Garmestani, H.; Tannenbaum, R. *Carbon* **2007**, *45*, 2037–2046.
(31) Smith, B. W.; Benes, Z.; Luzzi, D. E.; Fishcer, J. E.; Walters, D. A.; Casavant, M. J.; Schimdt, J.; Smalley, R. E. *Appl. Phys. Lett.* **2000**, *77*, 663–665.
(32) Park, C.; Wilkinson, J.; Banda, S.; Ounaies, Z.; Wise, K. E.; Sauti, G.; Lillehel, P. T.; Harrison, J. S. *J. Polym. Sci., Part B: Polym. Phys.* **2006**, *44*, 1751–1762.
(33) Yarin, A. L.; Koombhongse, S.; Reneker, D. H. *J. Appl. Phys.* **2001**, *89*, 3018–3026.
(34) Shin, Y. M.; Hohman, M. M.; Brenner, M. P.; Rutledge, G. C. *Appl. Phys. Lett.* **2001**, *78*, 1149–1151.
(35) Shin, Y. M.; Hohman, M. M.; Brenner, M. P.; Rutledge, G. C. *Polymer* **2001**, *42*, 9955–9967.
(36) Mazinani, S.; Ajji, A.; Dubois, C. *Polymer* **2009**, *50*, 3329–3342.
(37) McCullen, S. D.; Stevens, D. R.; Roberts, W. A.; Ojha, S. S.; Clarke, L. I.; Gorga, R. E. *Macromolecules* **2007**, *40*, 997–1003.
(38) Jeong, J. S.; Moon, J. S.; Park, J. H.; Alegaonkar, P. S.; Yoo, J. B. *Thin Solid Films* **2007**, *515*, 5136–5141.
(39) Wang, G.; Tan, Z.; Liu, X.; Chawda, S.; Koo, J.-S.; Samuilov, V.; Dudley, M. *Nanotechnology* **2006**, *17*, 5829–5835.
(40) Sundaray, B.; Subhramanian, V.; Natarajan, T. S.; Krishnamurthy, K. *Appl. Phys. Lett.* **2006**, *88*, 143114−1143114−3.
(41) Hou, H.; Ge, J. J.; Zeng, J.; Li, Q.; Reneker, D. H.; Greiner, A.; Cheng, S. Z. D. *Chem. Mater.* **2005**, *17*, 967–973.
(42) Mathew, G.; Hong, J. P.; Rhee, J. M.; Lee, H. S.; Nah, C. *Polym. Test.* **2005**, *24*, 712–717.
(43) Zhou, W.; Wu, Y.; Wei, F.; Luo, G.; Qian, W. *Polymer* **2005**, *46*, 12689–12695.
(44) Sung, J. H.; Kim, H. S.; Jin, H.-J.; Choi, H. J.; Chin, I.-J. *Macromolecules* **2004**, *37*, 9899–9902.
(45) Salaha, W.; Dror, Y.; Khalfin, R. L.; Cohen, Y.; Yarin, A. L.; Zussman, E. *Langmuir* **2004**, *20*, 9852–9855.
(46) Dror, Y.; Salalha, W.; Khalfin, R. L.; Cohen, Y.; Yarin, A. L.; Zussman, E. *Langmuir* **2003**, *19*, 7012–7020.
(47) Pham, T. A.; Kim, D. P.; Lim, T. W.; Park, S. H.; Yang, D. Y.; Lee, K. S. *Adv. Funct. Mater.* **2006**, *16*, 1235–1241.
(48) Wan, J.; Alizadeh, A.; Taylor, S. T.; Malenfant, P. R. L.; Manoharan, M.; Loureiro, S. M. *Chem. Mater.* **2005**, *17*, 5613–5617.
(49) Gupta, P.; Elkins, C.; Long, T. E.; Wilkes, G. L. *Polymer* **2005**, *46*, 4799–4810.
(50) Winter, G.; Verbeek, W.; Mansmann, M. U.S. Patent 3 892 583, 1975.
(51) Kenway, E. R.; Layman, J. M.; Watkins, J. R.; Bowlin, G. L.; Matthews, J. A.; Simpson, D. G. *Biomaterials* **2003**, *24*, 907–913.
(52) Shenoy, S. L.; Bates, W. D.; Frisch, H. L.; Wnek, G. E. *Polymer* **2005**, *46*, 3372–3384.
(53) Francois, B.; Pitois, O.; Francois, J. *Adv. Mater.* **1995**, *7*, 1041–1044.
(54) Li, Y.; Kroke, E.; Riedel, R.; Fasel, C.; Gervais, C.; Babonneau, F. *Appl. Organomet. Chem.* **2001**, *15*, 820–832.
(55) Hunley, M. T.; Pötschke, P.; Long, T. E. *Macromol. Rapid Commun.* **2009**, *30*, 2102–2106.
(56) Rosenhead, L. *Laminar Boundary Layers*: Clarendon Press: Oxford, U.K., 1963; 144−150.
(57) Stephan, C.; Nguyen, T. P.; Chapelle, M.; Lefrant, S.; Journet, C.; Bernier, P. *Synth. Met.* **2000**, *108*, 139–149.
(58) Du, F.; Fischer, J. E.; Winey, K. I. *Phys. Rev. B: Condens. Matter Mater. Phys.* **2005**, *72*, 121404−1121404−4.

AM1000085